International Journal of Thermal Sciences 54 (2012) 253–261

Contents lists available at SciVerse ScienceDirect

International Journal of Thermal Sciences

journal homepage: www.elsevier.com/locate/ijts

Effect of partial slip boundary condition on the flow and heat transfer of nanofluids past stretching sheet prescribed constant wall temperature

Aminreza Noghrehabadi*, Rashid Pourrajab, Mohammad Ghalambaz

Department of Mechanical Engineering, Shahid Chamran University of Ahvaz, Ahvaz, Iran

ARTICLE INFO

Article history:
Received 30 June 2011
Received in revised form
22 November 2011
Accepted 22 November 2011
Available online 29 December 2011

Keywords:
Nanofluid
Partial slip
Similarity solution
Stretching sheet
Constant wall temperature

ABSTRACT

The objective of the present study is to analyze the development of the slip effects on the boundary layer flow and heat transfer over a stretching surface in the presence of nanoparticle fractions. In the modeling of nanofluid the dynamic effects including the Brownian motion and thermophoresis are taken into account. In the case of constant wall temperature a similarity solution is presented. The solution depends on a Prandtl number, slip factor, Brownian motion number, Lewis number, and thermophoresis number. The dependency of the local Nusselt and local Sherwood numbers on these five parameters is numerically investigated. To the best of author's knowledge, the effects of slip boundary condition in the presence of dynamic effects of nano particles have not been investigated yet. The results of the present paper show the flow velocity and the surface shear stress on the stretching sheet and also reduced Nusselt number and reduced Sherwood number are strongly influenced by the slip parameter.

1. Introduction

Nanofluid is described as a fluid in which solid nanoparticles with the length scales of 1–100 nm are suspended in conventional heat transfer basic fluid. These nanoparticles enhance thermal conductivity and the convective heat transfer coefficient of the base fluid significantly. Conventional heat transfer fluids such as oil, water and ethylene glycol mixture are poor heat transfer fluids, because the thermal conductivity of these fluids affects the heat transfer coefficient between the heat transfer medium and the heat transfer surface. So many techniques have been taken to increase the thermal conductivity of these fluids by suspending nano/micro or large-sized particle materials in the liquid [1]. One of these techniques is the addition of nanoparticles to the base liquid [2]. As Choi et al. indicated for the first time, this method increased the thermal conductivity of the fluid up to approximately two times [3]. Then, Khanafer et al. studied heat transfer performance of nanofluids inside an enclosure [4].

Today nanotechnology is considered as a significant factor which affects the industrial revolution of the current century. Therefore, many researchers have focused on modeling the thermal conductivity and examined different viscosities of nanofluids over the past decade. In 2009, Kakac and Pramuanjaroenkij presented a comprehensive study of convective transport in nanofluids [1].

Flow of a viscous fluid past a stretching sheet is a classical problem in fluid dynamics [5]. Flow of a boundary layer over a stretching sheet, which occurs in several engineering processes, has become greatly important in the past decades. It has many practical applications especially in the field of metallurgy and chemical engineering such as extrusion of polymer, cooling of metallic plate, drawing of paper films, glass blowing, paper production, etc. [6–8]. For instance, in the extrusion of a polymer in a melt-spinning process, the polymer from the die is generally drawn and simultaneously stretched into a sheet which is then solidified through quenching or gradual cooling by direct contact with water [9,10]. The heat transfer rate in the boundary layer over stretching sheets is important, because in the mentioned applications the quality of the final product depends on the heat transfer rate between the stretching surface and the fluid during the cooling or heating process [11]. Therefore, the choice of a suitable cooling/heating liquid is essential as it has a direct impact on the rate of heat transfer.

For the first time Crane [5] studied the forced convection boundary layer flow over a stretching sheet. Then, the heat and mass transfer on a stretching sheet with suction or blowing on the solid boundary was investigated by Gupta and Gupta [12]. After these pioneering works, the flow field over a stretching surface has

* Corresponding author. Tel.: +98 916 312 8841.
E-mail addresses: a.r.noghrehabadi@scu.ac.ir, a.r.noghrehabadi@gmail.com (A. Noghrehabadi), r-pourrajab@mscstu.scu.ac.ir (R. Pourrajab), m.ghalambaz@gmail.com (M. Ghalambaz).

1290-0729/$ – see front matter © 2011 Elsevier Masson SAS. All rights reserved.
doi:10.1016/j.ijthermalsci.2011.11.017

drawn considerable attention, and a good number of literature in different fields including magnetic flows [13], different thermal and flow boundary conditions [14], micropolar fluids [15], nanofluids [16] and non Newtonian fluids [17,18] have been generated on this problem [19–27]. Mukhopadhyay et al. considered the effects of slip and heat transfer on the flow over an unsteady stretching surface [28]. Wang [29] reported that the partial slip between the fluid and the moving surface may occur in situations that the fluid is particulate such as emulsions, suspensions, foams and polymer solutions.

Kuznetsav and Nield conducted a study to evaluate the effect of nanoparticles on natural convection boundary layer flow past a vertical plate [30]. They prepared the simplest boundary conditions in which both temperature and nanoparticle fractions were constant along the wall. Bachok et al. examined the boundary layer flow of nanofluids over a moving surface in a flowing fluid [31].

In a recent paper, Khan and Pop used the model of Kuznetsov and Nield [30] to study the boundary layer flow of nanofluids past a stretching sheet prescribed a constant surface temperature [32] and convective boundary condition [33]. Before the work of Khan and Pop [32], Wang [34] had previously used a partial slip boundary condition to study the flow of a pure fluid over a stretching sheet. Sahoo and Do [35] examined the effects of partial slip on the steady flow of an incompressible, electrically conducting third grade fluid due to a stretching sheet.

It is reported that the presence of nanoparticles causes the slip velocity condition on the interface of fluid and solid boundary [36]. Bocquet and Barrat considered the effect of flow boundary conditions from nano to micro scales near the interfaces [37]. They briefly discussed the mechanisms of heat transfer, and the influence of surface slip on interface.

To the best of authors' knowledge there is not any investigation to address the effect of slip boundary condition on the heat transfer characteristics of nanofluid flow over stretching sheet. The present study aims to examine the effect of slip boundary condition in the presence of nanoparticles on the heat transfer characteristics of stretching sheet.

2. Governing equations

Consider a two-dimensional viscous flow of a nanofluid over a stretching surface, in which the flow is incompressible and steady state. The velocity of surface is linear and it can be represented as $U_w(x) = cx$. Here, c is a constant and x is the coordinate measured along the stretching surface. The coordinate system and scheme of the problem is shown in Fig. 1.

The nanofluid flows at $y = 0$, where y is the coordinate measured normal to the stretching surface.

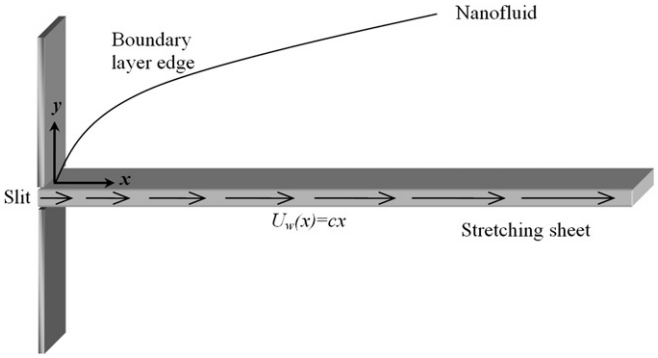

Fig. 1. Boundary layer configuration.

It is assumed that the wall temperature of T_w and the fraction of nanoparticles φ_w are constant at the stretching surface. When y attends to infinity, the ambient values of temperature and nanoparticle fraction attained to constant value of T_∞ and φ_∞ respectively. φ and T denote fraction of nanoparticles and temperature of flow respectively. In the laminar sublayer near the wall, Brownian diffusion and thermophoresis are important for nanoparticles of any material and size [38]. For nanofluids, in Cartesian coordinates system of x and y the governing steady conservation of momentum, thermal energy and nanoparticles equations including the dynamic effects of nanoparticles can be written as follows [20,39]

$$\frac{\partial u}{\partial x} + \frac{\partial v}{\partial x} = 0 \tag{1}$$

$$u\frac{\partial u}{\partial x} + v\frac{\partial u}{\partial y} = -\frac{1}{\rho_f}\frac{\partial p}{\partial x} + \upsilon\left(\frac{\partial^2 u}{\partial x^2} + \frac{\partial^2 u}{\partial y^2}\right) \tag{2}$$

$$u\frac{\partial v}{\partial x} + v\frac{\partial v}{\partial y} = -\frac{1}{\rho_f}\frac{\partial p}{\partial y} + \upsilon\left(\frac{\partial^2 v}{\partial x^2} + \frac{\partial^2 v}{\partial y^2}\right) \tag{3}$$

$$u\frac{\partial T}{\partial x} + v\frac{\partial T}{\partial y} = \alpha\left(\frac{\partial^2 T}{\partial x^2} + \frac{\partial^2 T}{\partial y^2}\right) + \tau\left\{D_B\left(\frac{\partial \varphi}{\partial x}\frac{\partial T}{\partial x} + \frac{\partial \varphi}{\partial y}\frac{\partial T}{\partial y}\right) + \frac{D_T}{T_\infty} \times \left[\left(\frac{\partial T}{\partial x}\right)^2 + \left(\frac{\partial T}{\partial y}\right)^2\right]\right\} \tag{4}$$

$$u\frac{\partial \varphi}{\partial x} + v\frac{\partial \varphi}{\partial y} = D_B\left(\frac{\partial^2 \varphi}{\partial x^2} + \frac{\partial^2 \varphi}{\partial y^2}\right) + \left(\frac{D_T}{T_\infty}\right)\left(\frac{\partial^2 T}{\partial x^2} + \frac{\partial^2 T}{\partial y^2}\right) \tag{5}$$

The boundary conditions for the velocity components with partial slip condition at the wall (*i.e.* $y = 0$) for nanoparticle fraction and temperature are defined as

$$v = 0, \quad u = U_w(x) - U_s, \quad T = T_w, \quad \varphi = \varphi_w, \quad \text{at } y = 0 \tag{6}$$

where considering Navier's condition the velocity slip is assumed to be proportional to the local shear stress [34]. The boundary conditions at the far filed (*i.e.* $y \to 0$) are defined as

$$v = u = 0, \quad T = T_\infty, \quad \varphi = \varphi_\infty, \quad \text{as } y \to \infty \tag{7}$$

Here, u and v are the velocity components along the axis x and y, respectively. p is the fluid pressure, α is the thermal diffusivity, υ is the kinematic viscosity, ρ_f is the density of the base fluid, ρ_p is the density of the particles, U_S is the velocity slip at the wall, D_B is the Brownian diffusion coefficient and D_T is the thermophoresis diffusion coefficient. $\tau = (\rho c)_p/(\rho c)_f$ is the ratio between the effective heat capacity of the nanoparticle material and heat capacity of the fluid with ρ being the density, φ is rescaled nanoparticle volume fraction.

To attain similarity solution of equations (1)–(5), the stream function and dimensionless variables can be posited in the following form

$$\psi = (c\upsilon)^{1/2} x f(\eta), \quad \eta = \left(\frac{c}{\upsilon}\right)^{1/2} y \tag{8-a}$$

$$\theta(\eta) = \frac{T - T_\infty}{T_w - T_\infty}, \quad \beta(\eta) = \frac{\varphi - \varphi_\infty}{\varphi_w - \varphi_\infty} \tag{8-b}$$

with these definitions, the velocities are expressed as $f'(\eta) = u/u_{w(x)}$ and the stream function ψ is defined with $u = \partial\psi/\partial y$, $v = -\partial\psi/\partial x$, so that (1) is satisfied identically. The pressure outside the boundary

layer (*i.e.* inviscid part of flow) is constant. Hence, the flow occurs only due to the stretching of the sheet; therefore, the pressure gradient can be neglected. By applying the similarity transforms on the remaining governing equations [*i.e.* (2)–(5)], the similarity equations are obtained as follows (see Appendix)

$$f''' + ff'' - f'^2 = 0, \tag{9}$$

$$\frac{1}{pr}\theta'' + f\theta' + \mathrm{Nb}\beta'\theta' + \mathrm{Nt}\theta'^2 = 0, \tag{10}$$

$$\beta'' + \frac{Nt}{Nb}\theta'' + Lef\beta' = 0, \tag{11}$$

Here, by using the boundary layer approximations and introducing the Navier's condition the velocity on the surface can be written as

$$u - U_{\mathrm{W}}(x) = N\rho\upsilon\frac{\partial u}{\partial y} = U_{\mathrm{S}} \tag{12}$$

where ρ is the density and N is a slip constant. By applying the similarity transforms, equation (12) reduces to

$$f'(0) - 1 = \lambda f''(0), \tag{13}$$

where $\lambda = N\rho(c\upsilon)^{1/2}$ is the dimensionless slip factor. Equations (9)–(11) can be solved numerically subject to the following boundary conditions

$$\text{At } \eta = 0 \quad : \quad f = 0, \quad f' = 1 + \lambda f'', \quad \theta = 1, \quad \beta = 1 \tag{14}$$

$$\text{At } \eta \to \infty \quad : \quad f' = 0, \quad \theta = 0, \quad \beta = 0 \tag{15}$$

where primes denote differentiation with respect to η. The parameters of Pr, Le, Nb and Nt are defined by

$$\mathrm{Pr} = \frac{\upsilon}{\alpha}, \ \mathrm{Le} = \frac{\upsilon}{D_{\mathrm{B}}}, \ \mathrm{Nb} = \frac{(\rho c)_{\mathrm{P}} D_{\mathrm{B}}(\varphi_{\mathrm{w}} - \varphi_\infty)}{(\rho c)_{\mathrm{f}}\upsilon}, \ \mathrm{Nt} = \frac{(\rho c)_{\mathrm{P}} D_{\mathrm{T}}(T_{\mathrm{w}} - T_\infty)}{(\rho c)_{\mathrm{f}}\upsilon T_\infty} \tag{16}$$

Here, Pr, Le, Nb and Nt denote the Prandtl number, the Lewis number, the Brownian motion parameter and the thermophoresis parameter, respectively. In the continuum modeling of fluidic transport, no slip boundary condition is sometimes assumed, that is the fluid velocity component is assumed to be zero relative to the solid boundary [40]. For nanofluids, however, this assumption no longer holds [40], and a certain degree of tangential slip must be allowed [36]. Indeed, nanofluidic flow usually exhibits partial slip against the solid surface, which can be characterized by the so-called slip length (around 3.4–68 mm for different liquids) [40].

Most nanofluids examined to date have large values for the Lewis number $\mathrm{Le} > 1$ [39]. For water nanofluids at room temperature with nanoparticles of 1–100 nm diameters, the Brownian diffusion coefficient D_{B} ranges from 4×10^{-4} to 4×10^{-12} m^2/s [38]. Furthermore, the ratio of Brownian diffusivity coefficient to thermophoresis coefficient for particles with diameters of 1–100 nm can be varied in the ranges of 2–0.02 for alumina, and from 2 to 20 for copper nanoparticles [38]. Khan and Pop [32] and Rana and Bhargava [41] as well as Makinde and Aziz [33] practically studied Nb and Nt in the range of 0.1–0.5 and Le in the range of 1–25 for the nanofluid boundary layer over the stretching sheets. Hence, the variation of non-dimensional parameters of nanofluids in the present study is considered to vary in the mentioned range.

In a case in which Nb and Nt are equal to zero, the present study reduces to the classical problem of flow and heat transfer due to a stretching surface in a viscous fluid. In this case, the boundary value problem for β becomes ill-posed without physical significance.

The quantities of local Nusselt number (Nu) and Sherwood number (Sh) as important parameters in heat transfer are given by

$$\mathrm{Nu} = \frac{xq_{\mathrm{w}}}{k(T_{\mathrm{w}} - T_\infty)}, \quad \mathrm{Sh} = \frac{xq_{\mathrm{m}}}{D_{\mathrm{B}}(\varphi_{\mathrm{w}} - \varphi_\infty)} \tag{17}$$

where q_{w} and q_{m} are the wall heat and mass fluxes, respectively.

Using similarity transforms in (8-a) and (8-b), one can obtain

$$\mathrm{Re}_x^{-1/2}\mathrm{Nu} = -\theta'(0), \quad \mathrm{Re}_x^{-1/2}\mathrm{Sh} = -\beta'(0) \tag{18}$$

where $\mathrm{Re}_x = u_{\mathrm{w}}(x)x/\upsilon$ is the local Reynolds number based on the stretching velocity $u_{\mathrm{w}}(x)$. Kuznetsov and Nield [20] referred $\mathrm{Re}_x^{-1/2}\mathrm{Nu}$ as the reduced Nusselt number, and the value of $\mathrm{Re}_x^{-1/2}\mathrm{Sh}$ as reduced Sherwood number. Furthermore, Khan and Pop used these parameters in their papers [32]. It is worth mentioning that Andersson [42] and Wang [29] obtained an exact solution for (9) subject to the boundary conditions (14) and (15).

3. Results and discussion

The set of ordinary differential equations of (9)–(11) are solved numerically for various range of slip boundary condition and for different values of the Prandtl number, the Lewis number, the Brownian motion parameter and the thermophoresis parameter.

Highly non-linear momentum boundary layer equation and thermal boundary layer equation are converted into similarity equations and then solved numerically by employing fifth order Runge–Kutta–Fehlberg scheme with shooting method [43]. The most crucial factor of this numerical solution is to choose the appropriate finite value of η_∞. Thus, the asymptotic boundary conditions given by (15) were replaced by a comparatively large value $\eta_{\max} = 15$ for the similarity variable ($\eta_{\max}$). The choice of $\eta_{\max} = 15$ ensured that all numerical solutions approached to the asymptotic values correctly. It is worth mentioning to consider that the selection of a large value for $\eta_{\max}$ is an important point that is often overlooked in publications on the boundary layer flows.

As a test of the accuracy of the solution, the values of $f''(0)$ and $f(\infty)$ are compared with analytical values reported by Wang [29,34] and Sahoo and Do [35] in Table 1. This table shows the numerical solution obtained by the present algorithm and the exact analytical solution reported by Wang [29,34] and Sahoo and Do [35] are in very good agreement.

Table 1
Comparison of results for the shear stress at surface $-f''(0)$ and $f(\infty)$ with the slip factor λ.

λ	$-f''(0)$			$f(\infty)$			
	Current result	Sahoo and Do [35]	Wang [29]	Current result	Sahoo and Do [35]	Wang [29]	Wang [34]
0.0	1.0	1.001154	1.0	1.0	1.001483	1.0	1.0
0.1	0.872082	0.871447	–	0.955401	0.955952	–	–
0.2	0.776377	0.774933	–	0.919088	0.919010	–	–
0.3	0.701548	0.699738	0.701	0.888557	0.888004	0.887	–
0.5	0.591195	0.589195	–	0.839284	0.838008	–	0.8393
1.0	0.430160	0.428450	0.430	0.754866	0.752226	0.748	0.7549
2.0	0.283980	0.282893	0.284	0.657249	0.652253	0.652	
3.0	0.214055	0.213314	–	0.598077	0.590892	–	0.5982
5.0	0.144841	0.144430	0.145	0.524839	0.513769	0.514	–
10	0.081243	0.081091	–	0.431976	0.413655	–	0.4331
20	0.043790	0.043748	0.0438	0.349358	0.322559	0.332	–

Table 2 compares results for the reduced Sherwood number (Shr) and the reduced Nusselt number (Nur) for Pr = 10, Le = 10 and no slip condition (*i.e.* $\lambda = 0$) obtained in the present work with those reported by Khan and Pop [32]. Consider that the zero value of slip factor simulates the stretching model used in the work of Khan and Pop [32]. Table 2 shows that the present results are in good agreement with the results reported by Khan and Pop [32].

Table 2
Comparison of results for the reduced Nusselt number $-\theta'(0)$ and reduced Sherwood number $-\beta'(0)$ when Le = Pr = 10 and $\lambda = 0$.

Nt	Nb	Nur (Khan and Pop [32])	Nur (present results)	Shr (Khan and Pop [32])	Shr (present results)
0.1	0.1	0.9524	0.9523768	2.1294	2.1293938
0.2	0.1	0.6932	0.6931743	2.2740	2.2740215
0.3	0.1	0.5201	0.5200790	2.5286	2.5286382
0.4	0.1	0.4026	0.4025808	2.7952	2.7951701
0.5	0.1	0.3211	0.3210543	3.0351	3.0351425
0.1	0.2	0.5056	0.5055814	2.3819	2.3818706
0.1	0.3	0.2522	0.2521560	2.4100	2.4100188
0.1	0.4	0.1194	0.1194059	2.3997	2.3996502
0.1	0.5	0.0543	0.0542534	2.3836	2.3835712

Tables 3 and 4 show the variation of the reduced Nusselt number (Nur) and reduced Sherwood number (Shr) respectively for different values of Nb, Nt and λ when Pr = 10 and Le = 10. It is observed that Nur is a decreasing function of dimensionless parameters of Pr, Le, Nb and Nt, while Shr is an increasing function of mentioned dimensionless parameters. However, both reduced Nusselt number and reduced Sherwood number are increasing functions of dimensionless parameter of λ. This means that by increasing the dimensionless slip parameter on the boundary the Nur and Shr will be decrease accordingly.

Velocity profiles $f'(\eta)$ and shear stress $f''(\eta)$ profiles for a variation of slip parameters λ are shown in Fig. 2 when Pr = 10, Le = 10, Nb = 0.5 and Nt = 0.5. This figure shows the effect of slip boundary condition on the velocity and shear stress in the flow field. It is seen that for increased slip λ the lateral velocity decreases near the surface but increases at larger distances. These results are in very good agreement with reported results by Wang [34]. The decrease in velocity at the surface is revealed the flow of fluid comes from stretching of the sheet; therefore any increase in slip of fluid on the stretching surface causes decrease in flow velocity profiles. Furthermore, it is observed that the magnitude of wall shear stress decreases with the increase of slip factor.

Table 3
Variation of Nur with Nb, Nt and λ for Le = Pr = 10.

Nb	Nt	$\lambda = 0$	$\lambda = 0.5$	$\lambda = 1$	$\lambda = 3$	$\lambda = 10$
0.1	0.1	0.952377	0.799317	0.718928	0.569705	0.412468
	0.2	0.693174	0.581772	0.523262	0.414652	0.300210
	0.3	0.520079	0.436495	0.392596	0.311077	0.225245
	0.4	0.402581	0.337881	0.303899	0.240821	0.174358
	0.5	0.321054	0.269457	0.242357	0.192053	0.139050
0.2	0.1	0.505581	0.424328	0.381652	0.302434	0.218955
	0.2	0.365358	0.306640	0.275801	0.218554	0.158230
	0.3	0.273096	0.229206	0.206154	0.163364	0.118275
	0.4	0.210984	0.177076	0.159267	0.126209	0.091376
	0.5	0.168077	0.141064	0.126877	0.100542	0.072795
0.3	0.1	0.252156	0.211631	0.190347	0.150837	0.109199
	0.2	0.181597	0.152412	0.137084	0.108630	0.078645
	0.3	0.135514	0.113735	0.102297	0.081064	0.058689
	0.4	0.104609	0.087797	0.078967	0.062576	0.045306
	0.5	0.083298	0.069911	0.062880	0.049829	0.036078

Table 4
Variation of Shr with Nb, Nt and λ when Le = Pr = 10.

Nb	Nt	$\lambda = 0$	$\lambda = 0.5$	$\lambda = 1$	$\lambda = 3$	$\lambda = 10$
0.1	0.1	2.129394	1.787171	1.607430	1.277377	0.922099
	0.2	2.274021	1.908555	1.716607	1.360282	0.984678
	0.3	2.528638	2.122251	1.908809	1.512585	1.094883
	0.4	2.795170	2.345948	2.110007	1.672014	1.210243
	0.5	3.035142	2.547353	2.291156	1.815555	1.314098
0.2	0.1	2.381871	1.99907	1.798019	1.424805	1.031454
	0.2	2.515223	2.11099	1.898684	1.504572	1.089178
	0.3	2.655459	2.228691	2.004545	1.588456	1.149881
	0.4	2.781777	2.334708	2.099898	1.664015	1.204555
	0.5	2.888339	2.424144	2.180339	1.727756	1.250672
0.3	0.1	2.410019	2.022696	1.819268	1.441643	1.043650
	0.2	2.514996	2.110803	1.898513	1.504438	1.089095
	0.3	2.608819	2.189547	1.969337	1.560559	1.129708
	0.4	2.687608	2.255673	2.028813	1.607688	1.163810
	0.5	2.751875	2.309612	2.077327	1.646130	1.191622

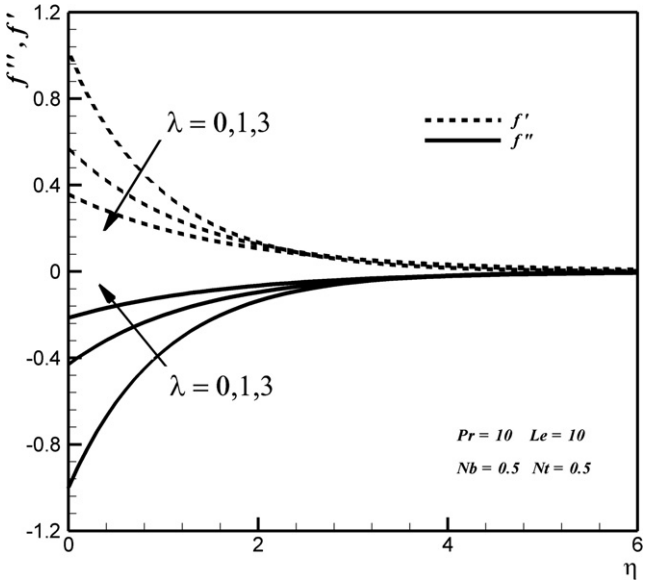

Fig. 2. Plots of dimensionless similarity functions $f'(\eta)$, $f''(\eta)$ for specified parameters.

For a typical case with Pr = 10, Le = 10, Nb = 0.1 and Nt = 0.1 which is used in the work of Khan and Pop [32], the dependent similarity variables $\theta(\eta)$ and $\varphi(\eta)$ are plotted for a variation of slip parameter of λ in Figs. 3 and 4 respectively. In these figures (*i.e.* Figs. 3 and 4) in the case of $\lambda = 0$ the zero value of slip factor simulates the stretching model used in the study of Khan and Pop [32]. Therefore, present solution is compared with the reported results by Khan and Pop [32]. As expected, in this case the thickness of the temperature boundary layer is smaller than thickness of

velocity boundary layer in Fig. 2. Also, as the parameter λ increases, the temperature of flow field increases for the specified parameters.

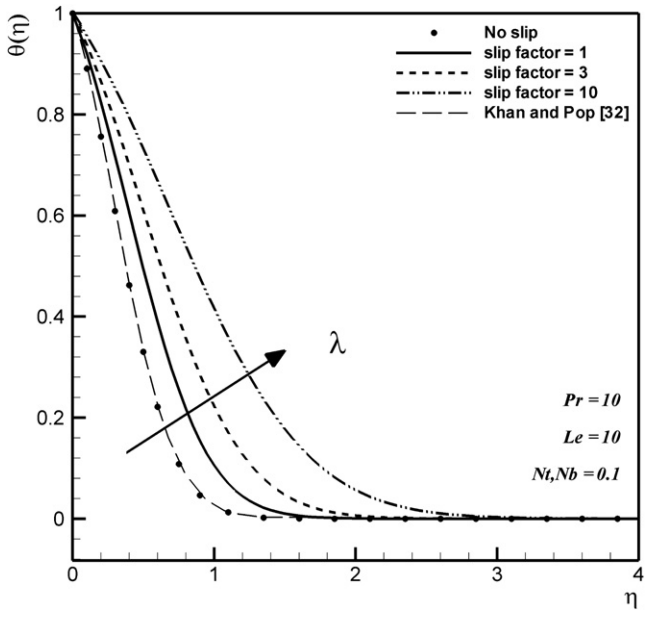

Fig. 3. Effect of λ on temperature distribution profiles for Pr = 10, Le = 10, Nt = 0.1 and Nb = 0.1.

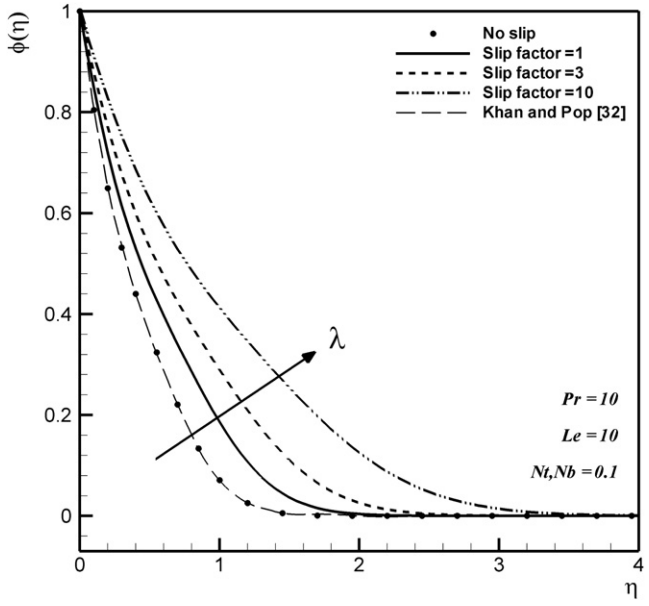

Fig. 4. Effect of λ on concentration distribution for Pr = 10, Le = 10, Nt = 0.1 and Nb = 0.1.

The profiles of concentration distribution for different values of parameter λ when $P = 10$, Le = 10, $N = 0.1$ and Nb = 0.1 are shown in Fig. 4. The profiles of concentration distribution increase with the increase in parameter λ.

The variation of dimensionless heat transfer rates (*i.e.* reduced Nusselt number) respect to Nt for different values of slip parameter of λ are shown in Figs. 5 and 6. For Figs. 5 and 6, the Prandtl numbers are equal to 1 and 10 respectively. These figures show the effects of Pr numbers and λ parameters on the dimensionless heat transfer rates for the same combination of Le, Nt and Nb those which are used in the work of Khan and Pop [32]. The case of $\lambda = 0$ simulates the no slip boundary condition. In the case of $\lambda = 0$ the obtained profiles of reduced Nusselt number are compared with results reported by Khan and Pop [32]. According to these figures (*i.e.* Figs. 5 and 6), the dimensionless heat transfer rates increase with the decrease in thermophoresis parameter or slip parameter of λ. It is also clear that reduced Nusselt number is increased with the increase of Pr number. A fluid with higher Prandtl number has a relatively lower thermal conductivity, which reduces conduction and thereby increases the heat transfer rate at the surface of the sheet.

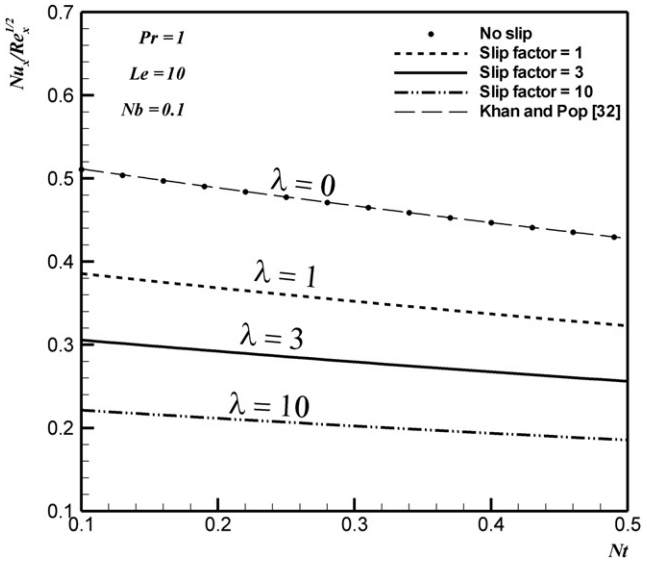

Fig. 5. Effects of λ and Nt on relation of reduced Nusselt number for Pr = 1, Le = 10 and Nb = 0.1.

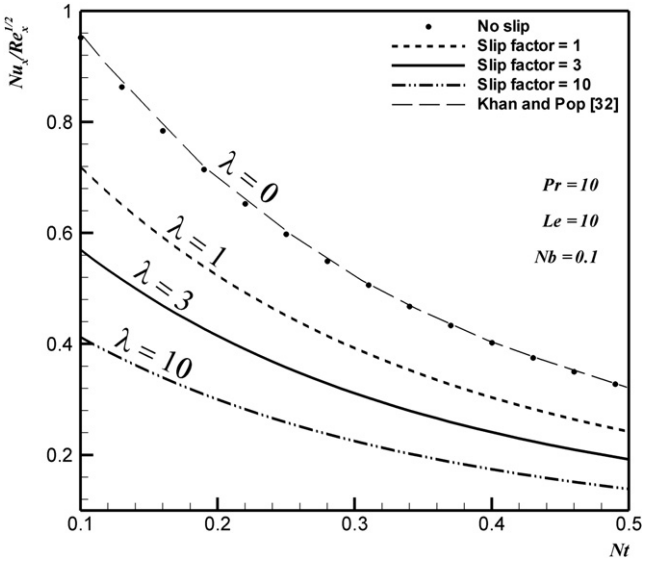

Fig. 6. Effects of λ and Nt on the relation of dimensionless reduced Nusselt number for Pr = 10, Le = 10 and Nb = 0.1.

The effect of slip boundary condition on the reduced Nusselt number for different values of Le = 5 and Le = 25 is shown in Figs. 7 and 8 respectively. Comparing these two figures shows that the change in the dimensionless heat transfer rates is higher for variation of slip parameters in smaller values of the thermophoresis parameter (Nt), and this change decreases with the increase of Nt. Also, the results of present work in the case of no slip flow boundary condition are compared with those reported by Khan and Pop [32].

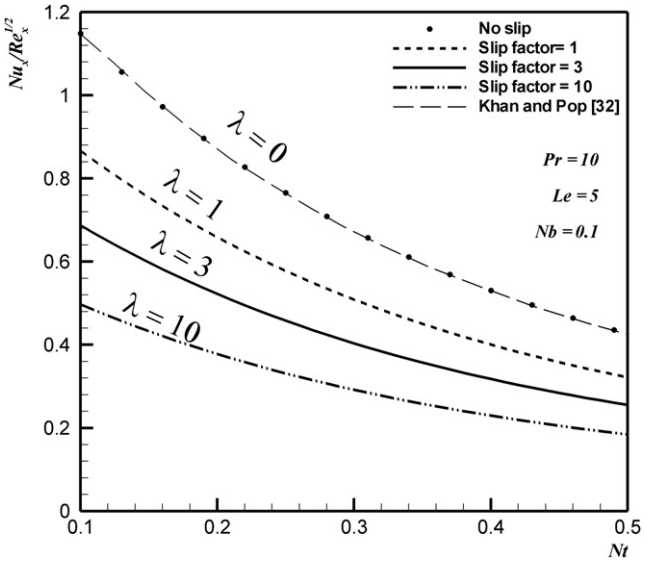

Fig. 7. Effects of λ and Nt on dimensionless heat transfer rates for Pr = 10, Le = 5 and Nb = 0.1.

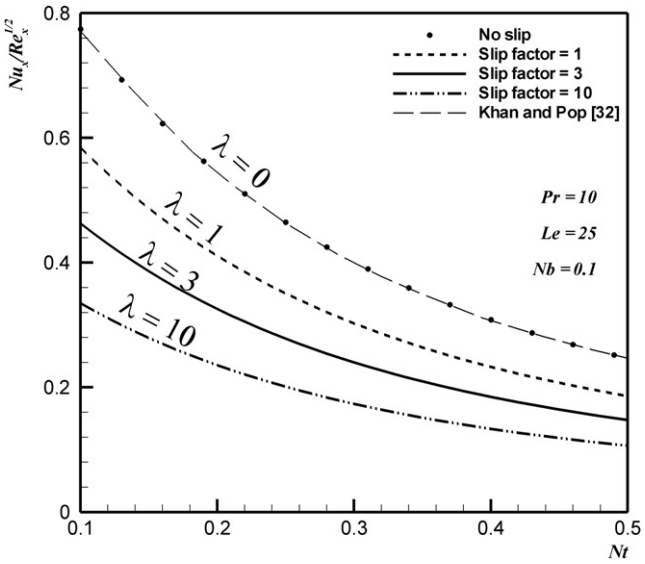

Fig. 8. Effects of λ and Nt on dimensionless heat transfer rates for Pr = 10, Le = 25 and Nb = 0.1.

Figs. 9 and 10 show the relation of reduced Sherwood (Shr) with thermophoresis parameter (Nt) for Pr = 1 and Pr = 10 respectively when Le = 10 and Nb = 0.3. It is clear from these figures that the dimensionless mass transfer rates with increase in thermophoresis parameter is decreased for small Pr numbers (*i.e.* Pr = 1) and slowly increased for large values of Prandtl number (*i.e.* Pr = 10). For both small and large Prandtl numbers, increase in slip parameter results in decrease in Shr number.

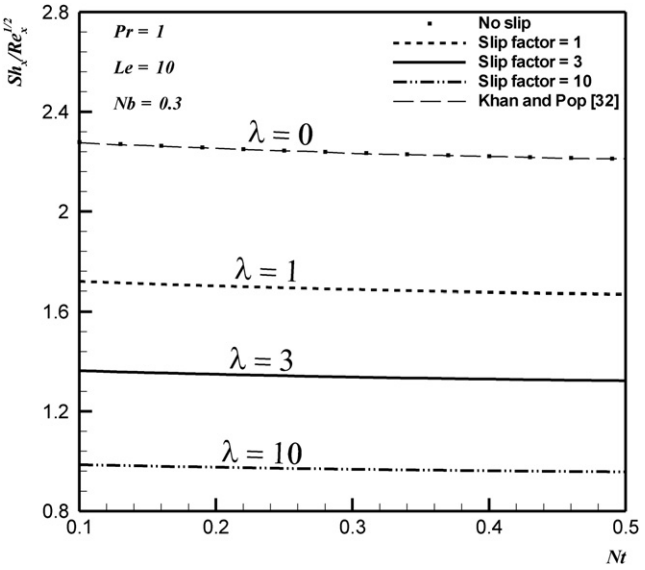

Fig. 9. Effects of λ and Nt on dimensionless concentration rates for Pr = 1, Le = 10 and Nb = 0.3.

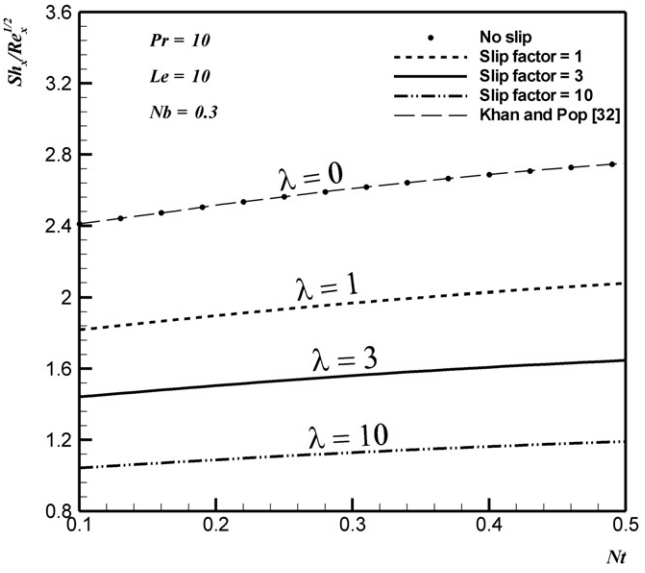

Fig. 10. Effects of λ and Nt on dimensionless concentration rates for Pr = 10, Le = 10 and Nb = 0.3.

Figs. 11 and 12 show the variation of reduced Sherwood (Shr) vs thermophoresis parameter (Nt) for Le = 5 and Le = 25 respectively when Pr = 10 and Nb = 0.2. These figures show that the dimensionless mass transfer rates increase with the increase in thermophoresis parameter for small and large values of Le numbers. It is observed that the increase of Lewis number increases the dimensionless mass transfer rates. In both small and large Lewis numbers any increase in slip parameter λ leads to decrease of Shr number.

Figs. 11 and 12 show for small and large values of Lewis number (*i.e.* Le = 5 and Le = 25) an increase of thermophoresis parameter causes the increase of the Shr monotonically.

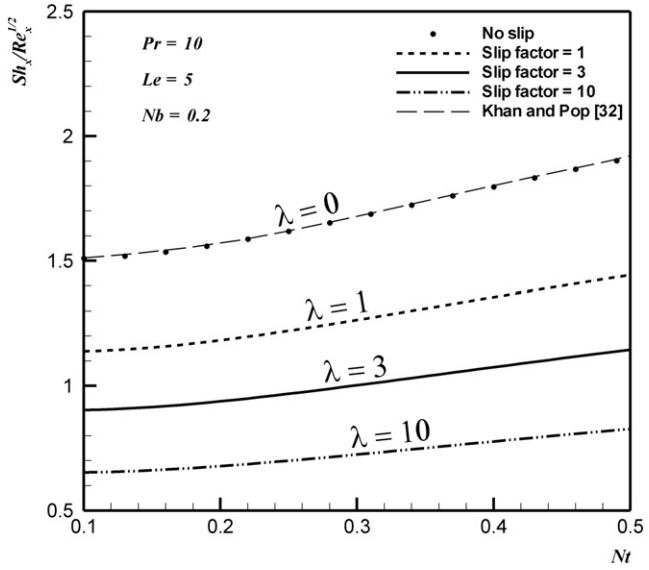

Fig. 11. Effects of λ and Nt on dimensionless concentration rates for Pr = 10, Le = 5 and Nb = 0.2.

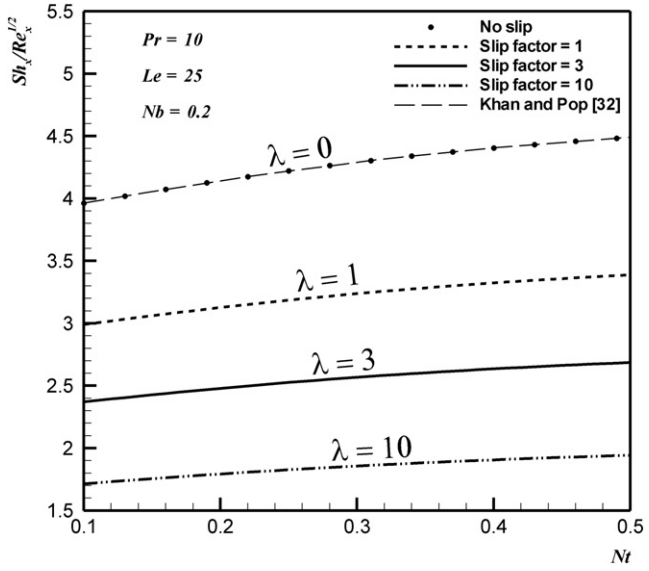

Fig. 12. Effects of λ and Nt on dimensionless concentration rates for Pr = 10, Le = 25 and Nb = 0.2.

Finally, in all cases a decrease in the dimensionless heat transfer rates was observed with the increase in slip parameter of λ.

4. Conclusion

In this paper, the effect of partial slip (*i.e.* Navier's condition) on the boundary layer flow and heat transfer of nanofluid past stretching sheet prescribe constant temperature is investigated. The boundary layer equations governing the flow are reduced to a set of non-linear ordinary differential equations using a similarity transformation. The obtained differential equations are solved numerically for different combinations of nanofluid parameters. Effect of slip parameter (λ) and nanofluid parameters including Lewis number (Le), Brownian motion number (Nb), thermophoresis number (Nt) on the momentum and thermal boundary layers are discussed using tables and figures. It is found that the flow velocity and the surface shear stress on stretching sheet are strongly influenced by the slip parameter. It is observed that by the increase in velocity slip factor (λ) the momentum boundary layer thickness and thermal boundary layer thickness decreased and increased respectively. The reduced Nusselt number and reduced Sherwood number are decreased with increase of velocity slip parameter (λ). We conclude that by the increase of thermophoresis number, the effect of velocity slip parameter on reduced Nusselt number and reduced Sherwood number increase and decrease respectively.

Appendix

By using the definition of ψ and taking P as a constant, the momentum equations (2) and (3) can be rewritten as,

$$\frac{\partial\psi}{\partial y}\frac{\partial^2\psi}{\partial y\partial x}-\frac{\partial\psi}{\partial x}\frac{\partial^2\psi}{\partial y^2}=\upsilon\left(\frac{\partial^3\psi}{\partial y\partial x^2}+\frac{\partial^3\psi}{\partial y^3}\right) \tag{A1}$$

Here, by using the introduce similarity variables of (8-a) and (8-b) each term of (A1) can be written as follows,

$$\frac{\partial f(\eta)}{\partial y}=\frac{\partial f}{\partial\eta}\frac{\partial\eta}{\partial y}=f'\left(\frac{c}{\upsilon}\right)^{1/2} \tag{A2}$$

$$\frac{\partial\psi}{\partial y}=(c\upsilon)^{1/2}x\frac{f(\eta)}{\partial y}=(c\upsilon)^{1/2}xf'\left(\frac{c}{\upsilon}\right)^{1/2}=f'cx \tag{A3}$$

$$\frac{\partial\psi}{\partial x}=(c\upsilon)^{1/2}f \tag{A4}$$

$$\frac{\partial^2\psi}{\partial y\partial x}=\frac{\partial}{\partial x}(f'cx)=cf' \tag{A5}$$

$$\frac{\partial^2\psi}{\partial y^2}=\frac{f'(\eta)}{\partial y}cx=cxf''\left(\frac{c}{\upsilon}\right)^{1/2} \tag{A6}$$

$$\frac{\partial^2\psi}{\partial x^2}=0,\quad \frac{\partial^3\psi}{\partial y\partial x^2}=0 \tag{A7}$$

$$\frac{\partial^3\psi}{\partial y^3}=cx\left(\frac{c}{\upsilon}\right)f''' \tag{A8}$$

By substituting (A3)–(A8) into (A1) the following equation obtained,

$$f'cx\times cf'-(c\upsilon)^{1/2}f\times cxf''\left(\frac{c}{\upsilon}\right)^{1/2}=\nu\left(0+cx\left(\frac{c}{\upsilon}\right)f'''\right) \tag{A9}$$

which can be simplified as,

$$f'''+ff''-f'^2=0, \tag{A10}$$

The introduced similarity variables of (8-b) can be rewritten as,

$$\theta(\eta)=\frac{T-T_\infty}{T_w-T_\infty},\quad T=\theta(\eta)(T_w-T_\infty)+T_\infty,\quad \beta(\eta)=\frac{\varphi-\varphi_\infty}{\varphi_w-\varphi_\infty},$$
$$\varphi=\beta(\eta)(\varphi_w-\varphi_\infty)+\varphi_\infty, \tag{A11}$$

Using (A11) each term of heat equation (4) can be evaluated as follow,

$$\frac{\partial T}{\partial x} = \frac{\partial T}{\partial \theta}\frac{\partial \theta}{\partial \eta}\frac{\partial \eta}{\partial x} = 0, \tag{A12}$$

$$\frac{\partial^2 T}{\partial x^2} = 0, \tag{A13}$$

$$\frac{\partial T}{\partial y} = \frac{\partial T}{\partial \theta}\frac{\partial \theta}{\partial \eta}\frac{\partial \eta}{\partial y} = \theta'(T_w - T_\infty)\left(\frac{c}{\upsilon}\right)^{1/2} \tag{A14}$$

$$\frac{\partial^2 T}{\partial y^2} = \theta''(T_w - T_\infty)\left(\frac{c}{\upsilon}\right), \tag{A15}$$

$$\frac{\partial \phi}{\partial x} = 0, \tag{A16}$$

$$\frac{\partial \phi}{\partial y} = \beta'(\varphi_w - \varphi_\infty)\left(\frac{c}{\upsilon}\right)^{1/2}, \tag{A17}$$

$$\frac{\partial^2 \phi}{\partial y^2} = \beta''(\varphi_w - \varphi_\infty)\left(\frac{c}{\upsilon}\right) \tag{A18}$$

By substituting (A12)–(A18) in (4) following equation is obtained,

$$\begin{aligned} 0 - (c\upsilon)^{1/2} f\theta'(T_w - T_\infty)\left(\frac{c}{\upsilon}\right)^{1/2} &= \alpha\theta''(T_w - T_\infty)\left(\frac{c}{\upsilon}\right) + \tau D_B \\ &\times \left(0 + \beta'(\varphi_w - \varphi_\infty)\left(\frac{c}{\upsilon}\right)^{1/2}\theta'\right. \\ &\times (T_w - T_\infty)\left(\frac{c}{\upsilon}\right)^{1/2}\Big) + \tau\frac{D_T}{T_\infty} \\ &\times \left(\theta'(T_w - T_\infty)\left(\frac{c}{\upsilon}\right)^{1/2}\right)^2 \end{aligned} \tag{A19}$$

where by dividing by $c \times (T_w - T_\infty)$ it can be simplified as follows,

$$-f\theta' = \frac{\alpha}{\upsilon}\theta'' + \frac{\tau D_B}{\upsilon}(\varphi_w - \varphi_\infty)\,\theta'\beta' + \frac{\tau D_T (T_w - T_\infty)}{T_\infty \upsilon}\theta'^2, \tag{A20}$$

$$\frac{1}{pr}\theta'' + f\theta' + \mathrm{Nb}\beta'\theta' + \mathrm{Nt}\theta'^2 = 0, \tag{A21}$$

where:

$$\mathrm{Pr} = \frac{\upsilon}{\alpha},\ \mathrm{Le} = \frac{\upsilon}{D_B},\ \mathrm{Nb} = \frac{(\rho c)_P D_B(\varphi_w - \varphi_\infty)}{(\rho c)_f \upsilon},\ \mathrm{Nt} = \frac{(\rho c)_P D_T (T_w - T_\infty)}{(\rho c)_f \upsilon T_\infty} \tag{A22}$$

By substituting (A12)–(A18) in (5) following equation is obtained,

$$\begin{aligned} 0 - (c\upsilon)^{1/2} f\beta'(\varphi_w - \varphi_\infty)\left(\frac{c}{\upsilon}\right)^{1/2} &= D_B\beta''(\varphi_w - \varphi_\infty)\left(\frac{c}{\upsilon}\right) \\ &+ \frac{D_T(T_w - T_\infty)}{T_\infty}\theta''\left(\frac{c}{\upsilon}\right), \end{aligned} \tag{A23}$$

where can be simplified as,

$$\beta'' + \frac{D_T}{T_\infty D_B}\frac{(T_w - T_\infty)}{(\varphi_w - \varphi_\infty)}\theta'' + \frac{\upsilon}{D_B}f\beta' = 0 \tag{A24}$$

$$\frac{\mathrm{Nt}}{\mathrm{Nb}} = \frac{D_T}{T_\infty D_B}\frac{(T_w - T_\infty)}{(\varphi_w - \varphi_\infty)},\quad \mathrm{Le} = \frac{\upsilon}{D_B} \tag{A25}$$

$$\beta'' + \frac{\mathrm{Nt}}{\mathrm{Nb}}\theta'' + \mathrm{Le}f\beta' = 0, \tag{A26}$$

References

[1] S. Kakaç, A. Pramuanjaroenkij, Review of convective heat transfer enhancement with nanofluids, Int. J. Heat Mass Transfer 52 (2009) 3187–3196.
[2] S.U.S. Choi, Enhancing thermal conductivity of fluids with nanoparticles, in: The Proceedings of the 1995 ASME International Mechanical Engineering Congress and Exposition, San Francisco, USA, ASME, FED 231/MD 66 (1995) pp. 99–105.
[3] S.U.S. Choi, Z.G. Zhang, W. Yu, F.E. Lockwood, E.A. Grulke, Anomalously thermal conductivity enhancement in nanotube suspensions, Appl. Phys. Lett. 79 (2001) 2252–2254.
[4] K. Khanafer, K. Vafai, M. Lightstone, Buoyancy-driven heat transfer enhancement in a two-dimensional enclosure utilizing nanofluids, Int. J. Heat Mass Transfer 46 (2003) 3639–3653.
[5] L.J. Crane, Flow past a stretching plate, J. Appl. Math. Phys. (ZAMP) 21 (1970) 645–647.
[6] Z. Tidmore, I. Klein, Engineering principles of plasticating extrusion, , In: Polymer Science and Engineering Series, Van Nostrand, New York, 1970.
[7] T. Altan, S. Oh, H. Gegel, Metal Forming Fundamentals and Applications, American Society of Metals, Metals Park, OH, 1979.
[8] E.G. Fisher, Extrusion of Plastics, Wiley, New York, 1976.
[9] V. Kumaran, A. Vanav Kumar, I. Pop, Transition of MHD boundary layer flow past a stretching sheet, Commun. Nonlinear Sci. Numer. Simulat. 15 (2010) 300–311.
[10] T.R. Mahapatra, A.S. Gupta, Magnetohydrodynamic stagnation-point flow towards a stretching sheet, Acta Mech. 152 (2001) 191–196.
[11] M.V. Karwe, Y. Jaluria, Numerical simulation of thermal transport associated with a continuous moving flat sheet in materials processing, ASME J. Heat Transfer 113 (1991) 612–619.
[12] P.S. Gupta, A.S. Gupta, Heat and mass transfer on a stretching sheet with suction or blowing, Can. J. Chem. Eng. 55 (1977) 744–746.
[13] K.V. Prasad, K. Vajravelu, P.S. Dutt, The effects of variable fluid properties on the hydro-magnetic flow and heat transfer over a non-linearly stretching sheet, Int. J. Therm. Sci. 40 (2010) 603–610.
[14] M. Turkyilmazoglu, Multiple solutions of heat and mass transfer of MHD slip flow for the viscoelastic fluid over a stretching sheet, Int. J. Therm. Sci. 50 (2011) 2264–2276.
[15] T. Hayat, T. Javed, Z. Abbas, MHD flow of a micropolar fluid near a stagnation-point towards a non-linear stretching surface, Nonlinear Anal. Real World Appl. 10 (2009) 1514–1526.
[16] K. Vajravelu, K.V. Prasad, Jinho Lee, Changhoon Lee, I. Pop, Robert A. Van Gorder, Convective heat transfer in the flow of viscous Ag–water and Cu–water nanofluids over a stretching surface, Int. J. Therm. Sci. 50 (2011) 843–851.
[17] F. Labropulu, D. Li, I. Pop, Non-orthogonal stagnation-point flow towards a stretching surface in a non-Newtonian fluid with heat transfer, Int. J. Therm. Sci. 49 (2010) 1042–1050.
[18] T. Hayat, M. Mustafa, S. Mesloub, Mixed convection boundary layer flow over a stretching surface filled with a Maxwell fluid in presence of Soret and Dufour effects, Z. Naturforsch. 65A (2010) 401–410.
[19] K.N. Lakshmisha, S. Venkateswaran, G. Nath, Three-dimensional unsteady flow with heat and mass transfer over a continuous stretching surface, ASME J. Heat Transfer 110 (1988) 590–595.
[20] C.Y. Wang, The three-dimensional flow due to a stretching flat surface, Phys. Fluids 27 (1984) 1915–1917.
[21] H.I. Andersson, B.S. Dandapat, Flow of a power-law fluid over a stretching sheet, Stab. Appl. Anal. Cont. Media 1 (1991) 339–347.
[22] M. Subhas Abel, Sujit Kumar Khan, K.V. Prasad, Study of visco-elastic fluid flow and heat transfer over a stretching sheet with variable viscosity, Int. J. Non-Linear Mech. 37 (2002) 81–88.
[23] K.V. Prasad, Subhas Abel, P.S. Datti, Diffusion of chemically reactive species of a non-Newtonian fluid immersed in a porous medium over a stretching sheet, Int. J. Non-Linear Mech. 38 (2003) 651–657.
[24] E.M. Sparrow, J.P. Abraham, Universal solutions for the stream wise variation of the temperature of a moving sheet in the presence of a moving fluid, Int. J. Heat Mass Transfer 48 (2005) 3047–3056.
[25] Rafael Cortell, Flow and heat transfer of an electrically conducting fluid of second grade over a stretching sheet subject to suction and to a transverse magnetic field, Int. J. Heat Mass Transfer 49 (2006) 1851–1856.
[26] J.P. Abraham, E.M. Sparrow, Friction drag resulting from the simultaneous imposed motions of a free stream and its bounding surface, Int. J. Heat Fluid Flow 26 (2005) 289–295.
[27] T. Hayat, T. Javed, M. Sajid, Analytic solution for MHD rotating flow of a second grade fluid over a shrinking surface, Phys. Lett. A 372 (2008) 3264–3273.
[28] S. Mukhopadhyay, H. Andersson, Effects of slip and heat transfer analysis of flow over an unsteady stretching surface, Int. J. Heat Mass Transfer 45 (2009) 1447–1452.

[29] C.Y. Wang, Flow due to a stretching boundary with partial slip-an exact solution of the Navier–Stokes equations, Chem. Eng. Sci. 57 (2002) 3745–3747.
[30] A.V. Kuznetsov, D.A. Nield, Natural convective boundary-layer flow of a nanofluid past a vertical plate, Int. J. Therm. Sci. 49 (2010) 243–247.
[31] N. Bachok, A. Ishak, I. Pop, Boundary-layer flow of nanofluids over a moving surface in a flowing fluid, Int. J. Therm. Sci. 49 (2010) 1663–1668.
[32] W.A. Khan, I. Pop, Boundary-layer flow of a nanofluid past a stretching sheet, Int. J. Heat Mass Transfer 53 (2010) 2477–2483.
[33] O.D. Makinde, A. Aziz, Boundary layer flow of a nanofluid past a stretching sheet with a convective boundary condition, Int. J. Therm. Sci. 50 (2011) 1326–1332.
[34] C.Y. Wang, Analysis of viscous flow due to a stretching sheet with surface slip and suction, Nonlinear Anal. Real World Appl. 10 (1) (2009) 375–380.
[35] B. Sahoo, Y. Do, Effects of slip on sheet-driven flow and heat transfer of a third grade fluid past a stretching sheet, Int. Commun. Heat Mass Transfer 37 (2010) 1064–1071.
[36] R.A. Van Gorder, E. Sweet, K. Vajravelu, Nano boundary layers over stretching surfaces, Commun. Nonlinear Sci. Numer. Simulat. 15 (2010) 1494–1500.
[37] L. Bocquet, J.L. Barrat, Flow boundary conditions from nano- to micro-scales, Soft Matter 3 (2007) 685–693.
[38] J. Buongiorno, Convective transport in nanofluids, ASME J. Heat Transfer 128 (2006) 240–250.
[39] D.A. Nield, A.V. Kuznetsov, The Cheng–Minkowycz problem for natural convective boundary layer flow in a porous medium saturated by a nanofluid, Int. J. Heat Mass Transfer 52 (2009) 5792–5795.
[40] M. Majumder, N. Chopra, R. Andrews, B.J. Hinds, Nanoscale hydrodynamics: enhanced flow in carbon nanotubes, Nature 438 (2005) 44.
[41] P. Rana, R. Bhargava, Flow and heat transfer of a nanofluid over a nonlinearly stretching sheet: a numerical study, Commun. Nonlinear Sci. Numer. Simulat. 17 (2012) 212–226.
[42] H.I. Andersson, Slip flow past a stretching surface, Acta Mech. 158 (2002) 121–125.
[43] T.Y. Na, Computational Method in Engineering Boundary Value Problems, Academic Press, New York, 1979.

Nomenclature

$(\rho c)_f$: heat capacity of the fluid
$(\rho c)_p$: effective heat capacity of the nanoparticle material
c: constant
D_B: Brownian diffusion coefficient
D_T: thermophoretic diffusion coefficient
k: thermal conductivity
Le: Lewis number
N: slip constant
Nb: Brownian motion parameter
Nt: thermophoresis parameter
Nu: Nusselt number
p: pressure
Pr: Prandtl number
q_m: wall mass flux
q_w: wall heat flux
Re_x: local Reynolds number
Sh_x: local Sherwood number
T: fluid temperature
T_∞: ambient temperature
T_w: temperature at the stretching sheet
u,v: velocity components along x- and y-axes
US: slip velocity at the wall
u_w: velocity of the stretching sheet
x,y: Cartesian coordinates (x-axis is aligned along the stretching surface and y-axis is normal to it)

Greek
α: thermal diffusivity
β: dimensionless nanoparticle volume fraction
η: similarity variable
θ: dimensionless temperature
λ: dimensionless slip factor
ρ_f: fluid density
ρ_p: nanoparticle mass density
τ: parameter defined by ratio between the effective heat capacity of the nanoparticle material and heat capacity of the fluid
υ: kinematics viscosity of fluid
φ: nanoparticle volume fraction
φ_∞: ambient nanoparticle volume fraction
φ_w: nanoparticle volume fraction at the stretching sheet
ψ: stream function